Polynomial Chirplet Transform With Application to Instantaneous Frequency Estimation

Z. K. Peng, G. Meng, F. L. Chu, Z. Q. Lang, W. M. Zhang, and Y. Yang

***Abstract*—In this paper, a new time–frequency analysis method known as the polynomial chirplet transform (PCT) is developed by extending the conventional chirplet transform (CT). By using a polynomial function instead of the linear chirp kernel in the CT, the PCT can produce a time–frequency distribution with excellent concentration for a wide range of signals with a continuous instantaneous frequency (IF). In addition, an effective IF estimation algorithm is proposed based on the PCT, and the effectiveness of this algorithm is validated by applying it to estimate the IF of a signal with a nonlinear chirp component and seriously contaminated by a Gaussian noise and a vibration signal collected from a rotor test rig.**

***Index Terms*—Chirplet transform (CT), instantaneous frequency (IF), polynomial chirplet transform (PCT), short-time Fourier transform (STFT), time–frequency analysis.**

I. Introduction

THE CONTROVERSIAL concept of instantaneous frequency (IF) was first put forward by Carson and Fry [1] in 1937 for the analysis of monocomponent frequency-modulated (FM) signals and then was further developed by Van der Pol [2] and Gabor [3]. Now, the widely acknowledged definition of the IF was proposed by Ville [4], unifying the work by Carson and Fry [1] and Gabor [3]. According to the definition of Ville, the IF of a signal can be calculated from the derivative of the phase of its analytic signal.

The IF concept has played important roles for the study of a wide range of signals, from radar [5], sonar [6], biomedical engineering [7], seismic investigation [8], and speech and music[9] to automotive signals [10], where the IFs are often used to characterize important physical parameters of the signals. Various IF estimation methods have been developed; Boashash [11], [12] contributed a comprehensive overview for these where the interpretation of the IF concept itself, as well as the literature about IF estimation methods published before 1992, was presented. Generally, the IF estimation methods can be classified into five categories: 1) phase difference-based IF estimators; 2) zero-crossing IF estimators; 3) linear-prediction-filter-based adaptive IF estimators; 4) IF estimators based on the moments of time–frequency distributions (TFDs); and 5) IF estimators based on the peak of TFDs. Among the five classes of the IF estimators, the use of TFDs can produce results that are more reliable and more robust to noise. Therefore, the TFD-based methods have attracted much more attention and developed more quickly than the others.

The capability of the TFD-based methods lies on the property of TFDs of concentrating the energy of a signal at and around the IF, in the time–frequency plane. Three approaches, namely, the short-time Fourier transform (STFT) [13], the continuous wavelet transform (CWT) [14], [15], and the Wigner–Ville distribution (WVD) [16], are commonly used to produce the TFDs for signals. The STFT and the CWT are essentially a kind of linear transforms characterized by a static resolution in the time–frequency plane, which is subdivided into elementary cells of a constant area. However, due to the restriction of the Heisenberg–Gabor inequality, neither the STFT nor the CWT is able to achieve a fine resolution in both the time and frequency domains, a good time resolution definitely implying a poor frequency resolution. Consequently, the time–frequency representation obtained by the two methods is meaningful only under a certain time/frequency resolution. Therefore, the STFT and CWT can never produce the true time–frequency pattern for a signal and so can only present an estimation of limited measurement accuracy to the IF for a signal, particularly when the IF trajectory is a nonlinear function of time. To improve the estimation accuracy, reassignment techniques [17] have been proposed. The WVD is a kind of quadratic transform that can achieve a highly accurate estimation for noise-free signals. When a signal has a linear frequency law and constant amplitude, its WVD will reduce to a row of delta functions along the linear IF trajectory. However, in the cases of noisy signals or nonlinear IF law, the WVD peak-based estimators would be biased, and it has been shown that the bias-to-variance tradeoff is inevitable for the estimated IF result. The bias caused by the IF nonlinearity is proportional to a power of the lag window length, while the variance caused by the noise is a decreasing function of the lag window length. Efforts have been made to improve the capability of the WVD to achieve a better estimation for the nonlinear IF, mainly through adjusting the window length. Stankovic and Katkovnik [18] suggested a method using

Manuscript received October 25, 2010; revised February 11, 2011; accepted February 12, 2011. Date of publication March 28, 2011; date of current version August 10, 2011. This work was supported in part by the Program for New Century Excellent Talents (NCET) in the University of China under Grant NCET-10-0548, by the Natural Science Foundation of China under Grants 10902068 and 10732060, by the Research Fund of the State Key Laboratory of Mechanical System and Vibration (MSV), China, under Grant MSV-ZD-2010-01, and by the Shanghai Pujiang Program under Grant 10PJ1406000. The Associate Editor coordinating the review process for this paper was Prof. Alessandro Ferrero.

Z. K. Peng, G. Meng, W. M. Zhang, and Y. Yang are with the State Key Laboratory of Mechanical System and Vibration, School of Mechanical Engineering, Shanghai Jiao Tong University, Shanghai 200240, China.

F. L. Chu is with Department of Precision Instruments and Mechanology, Tsinghua University, Beijing 100084, China (e-mail: chufl@mail.tsinghua.edu.cn).

Z. Q. Lang is with the Department of Automatic Control and Systems Engineering, University of Sheffield, S1 3JD Sheffield, U.K.

Color versions of one or more of the figures in this paper are available online at http://ieeexplore.ieee.org.

Digital Object Identifier 10.1109/TIM.2011.2124770

the WVD with an adaptive window length, and the same authors also proposed a way by using the WVD with varying and data-driven window length [19]. The TFD peak-based algorithm has also be applied in other WVD representations, including the polynomial WVD [20], [21], which was shown to be unbiased for the nonlinear IF trajectory, and the pseudo- and smoothed-pseudo-WVDs [22], which were intended to suppress the cross-terms caused by noise in the time–frequency plane.

Aside from the TFD analysis methods mentioned earlier, the chirplet transform (CT) [23] is another kind of TF method which is particularly designed for the analysis of chirplike signals with linear IF law. When the IF trajectory of the signal under consideration is a nonlinear function of time, the CT can no longer assure an enhancement of the analysis accuracy, and therefore Chassande-Mottin and Pai [24] suggested the chirplet chain to deal with the gravitational wave signals which essentially are a quasi-periodic FM signal, and Angrisani and D'Arco [25] proposed a modified version of the CT by introducing an extra curvature parameter to the conventional CT which was shown to be particularly effective for the signals with IF characterized by higher dynamics. In this paper, a new CT known as polynomial CT (PCT) is proposed. Based on the PCT, a procedure is then developed to estimate the IF of the signals with a highly nonlinear IF trajectory. The PCT is developed by replacing the chirplet kernel with a linear IF law in the CT with a new kernel with a polynomial nonlinear IF law. In mathematics, the Weierstrass approximation theorem [26] guarantees that any continuous function on a bounded interval can be uniformly approximated by a polynomial to any degree of accuracy. Therefore, the PCT is capable of presenting a highly accurate analysis for a wide range of signals with IF trajectories being any continuous functions of time.

This paper is organized as follows. After a brief description of the theory underlying the conventional CT, the details concerning the PCT are given in Section II. The PCT-based IF estimation procedure is then set up in Section III. In Section IV, the effectiveness of the new proposed IF estimator is validated by applying it to several signals. The conclusions are given in Section V.

II. Theoretical Background

A. Conventional CT

The CT [23], [27] of a signal $s(t) \in L^2(R)$ is defined as

$$CT_s(t_0,\omega,\alpha;\sigma) = \int_{-\infty}^{+\infty} z(t)\Psi^*_{(t_0,\alpha,\sigma)}(t)\exp(-j\omega t)\,dt \quad (1)$$

where $z(t)$ is the analytical signal of $s(t)$, generated by the Hilbert transform $\boldsymbol{H}$, i.e., $z(t) = s(t) + j\boldsymbol{H}[s(t)]$, and $\Psi^*_{(t_0,\alpha,\sigma)}(t)$ is a complex window given by

$$\Psi_{(t_0,\alpha,\sigma)}(t) = w_{(\sigma)}(t-t_0)\exp\left(-j\frac{\alpha}{2}(t-t_0)^2\right). \quad (2)$$

Here, the parameters t_0, $\alpha \in R$ stand for the time and chirp rate, respectively; $w \in L^2(R)$ denotes a nonnegative, symmetric, and normalized real window, usually taken as the Gaussian function expressed as

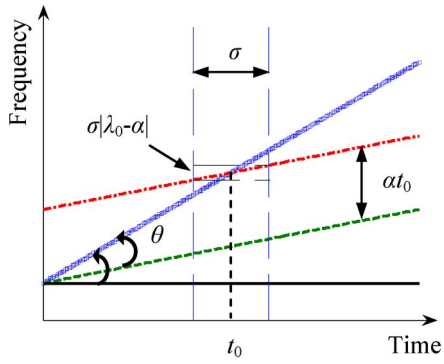

Fig. 1. Illustration of the conventional CT (□—the IF law of the object chirp signal; −—after frequency rotation; −.—after frequency shift).

$$w_{(\sigma)}(t) = \frac{1}{\sqrt{2\pi}\sigma}\exp\left(-\frac{1}{2}\left(\frac{t}{\sigma}\right)^2\right). \quad (3)$$

From the definition of the CT given as (1), the CT may be interpreted as the STFT of the analytical signal multiplied by the complex window $\Psi^*_{(t_0,\alpha,\sigma)}(t)$. The definition of the CT can also be written as

$$CT_s(t_0,\omega,\alpha;\sigma) = A(t_0)\int_{-\infty}^{+\infty} \bar{z}(t)w_{(\sigma)}(t-t_0)\exp(-j\omega t)\,dt \quad (4)$$

with

$$\begin{cases} \bar{z}(t) = z(t)\Phi^R_\alpha(t)\Phi^M_\alpha(t,t_0) \\ \Phi^R_\alpha(t) = \exp(-j\alpha t^2/2) \\ \Phi^M_\alpha(t,t_0) = \exp(j\alpha t_0 t) \\ A(t_0) = \exp\left(-jt_0^2\alpha/2\right). \end{cases} \quad (5)$$

Clearly, $\Phi^R_\alpha(t)$ is a frequency rotating operator which rotates the analytical signal $z(t)$ by an angle θ with $tg(\theta) = -\alpha$, in the time–frequency plane; $\Phi^M_\alpha(t,t_0)$ is the frequency shift operator that relocates a frequency component at ω to $\omega + \alpha t_0$; and $A(t_0)$ is a complex number with modulus $|A(t_0)| = 1$. In the time–frequency analysis, it is the modulus of the TFD $|CT_s(t_0,\omega,\alpha;\sigma)|$ that is usually of interest and meaningful, and therefore, the definition of the CT can be simplified as

$$CT_s(t_0,\omega,\alpha;\sigma) = \int_{-\infty}^{+\infty} \bar{z}(t)w_{(\sigma)}(t-t_0)\exp(-j\omega t)\,dt. \quad (6)$$

From this definition, it can be seen that the CT can be decomposed into a series of operators: 1) rotating the signal under consideration by a degree $\arctan(-\alpha)$ in the time–frequency plane; 2) shifting the signal by a frequency increment of αt_0; and 3) doing STFT with window $w_{(\sigma)}$. This procedure can be illustrated by Fig. 1, where the object chirp signal is with IF law of $\omega_0 + \lambda_0 t$.

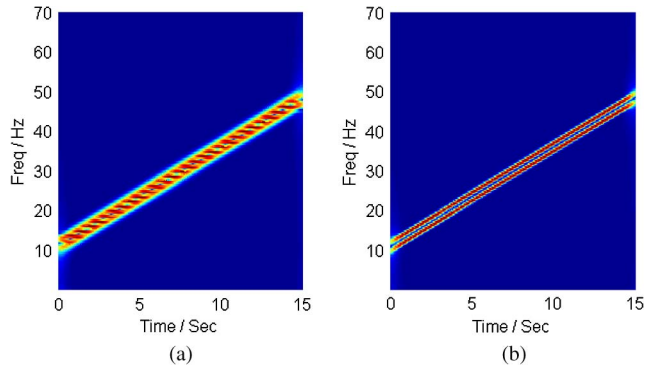

Fig. 2. TFDs generated by the CTs (window size = 512). (a) $\lambda_0 = 0$. (b) $\lambda_0 = 5\pi$.

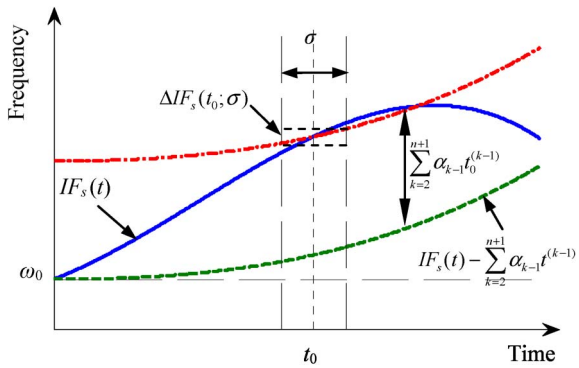

Fig. 3. Illustration of the PCT.

The frequency resolution of the CT can be easily determined from Fig. 1. If the chirp rate parameter $\alpha = 0$, the CT is equal to the normal STFT, and the frequency bandwidth of the signal portion selected by the Gaussian window with time bandwidth σ is $\sigma\lambda_0$; then, in the time–frequency plane, this signal portion would be presented as a cell of frequency bandwidth $\sigma\lambda_0 + 1/\sigma$ ($1/\sigma$ is the frequency bandwidth of the Gaussian window) and time bandwidth σ. In the case of $\alpha \neq 0$, the frequency bandwidth of the selected signal portion will reduce to $\sigma|\lambda_0 - \alpha| + 1/\sigma$, and the time bandwidth will be kept unchanged. It can be seen that, when $\alpha = \lambda_0$, the frequency bandwidth will have a minimum value $1/\sigma$; this implies that the TFD generated by the CT possesses the best concentration. Therefore, $|CT_s(t_0, \omega, \alpha; \sigma)|$ has global maximum at $(\omega, \alpha) = (\omega_0, \lambda_0)$.

Consider an example where the CT is applied to a signal consisting of two components, among which one is with IF law $10 + 2.5t$ (Hz) and the IF law of the other one is $12 + 2.5t$ (Hz), i.e.,

$$s(t) = \sin\left(2\pi(10 + 2.5t)t\right) + \sin\left(2\pi(12 + 2.5t)t\right) \quad (0 \le t \le 15 \text{ s}). \quad (7)$$

The signal is sampled at a sampling frequency of 200 Hz. Two different chirp rates are used, i.e., $\lambda_0 = 0$ and $\lambda_0 = 5\pi$. The results are shown in Fig. 2(a) and (b), respectively. It can be seen that, when $\lambda_0 = 0$, the CT is degenerated to the normal STFT, and the two components cannot be separated in the TFD shown in Fig. 2(a) because of the large frequency bandwidth; on the contrary, as indicated by Fig. 2(b), the two components show themselves off clearly in the time–frequency plane as in this case, and the concentration of the TFD is significantly improved because the chirp rate parameter used in the CT is properly selected to match the chirp rate of the signal under consideration.

B. PCT

As indicated by the example in Section II-A and some applications presented by other researchers, when the chirp rate is properly selected, the conventional CT would render the TFDs of an excellent concentration for the signals whose IF trajectory is a linear function of time. However, when the IF trajectory of a signal is not exactly a linear function of time, then it is impossible for the conventional CT to track the evolution versus time of the IF of the signal as closely as in Fig. 2(b). This is particularly true in the presence of IF characterized by highly nonlinear dynamics where a linear approximation is not adequate to locally represent the IF trajectory. To improve the efficacy of the conventional CT in analyzing the signals with a nonlinear IF trajectory, a modified version known as the PCT is proposed in this paper. The PCT is defined as follows:

$$PCT_s(t_0, \omega, \alpha_1, \ldots, \alpha_n; \sigma) = \int_{-\infty}^{+\infty} z(t)\Phi^R_{\alpha_1,\ldots,\alpha_n}(t) \times \Phi^M_{\alpha_1,\ldots,\alpha_n}(t, t_0) w_{(\sigma)}(t - t_0)\exp(-j\omega t)\, dt \quad (8)$$

with

$$\Phi^R_{\alpha_1,\ldots,\alpha_n}(t) = \exp\left(-j\sum_{k=2}^{n+1}\frac{1}{k}\alpha_{k-1}t^k\right) \quad (9)$$

$$\Phi^M_{\alpha_1,\ldots,\alpha_n}(t, t_0) = \exp\left(j\sum_{k=2}^{n+1}\alpha_{k-1}t_0^{(k-1)}t\right) \quad (10)$$

which are the nonlinear frequency rotating operator and the frequency shift operator, respectively, and $(\alpha_1, \ldots, \alpha_n)$ are the polynomial kernel characteristic parameters. The operating principle of the PCT can be illustrated as shown in Fig. 3, where $IF_s(t)$ is the IF trajectory of the signal under consideration. Specifically, the signal is first rotated in the time–frequency plane by subtracting from the IF of the signal, $IF_s(t)$, the IF of the nonlinear chirp kernel, i.e., $\sum_{k=2}^{n+1}\alpha_{k-1}t^{(k-1)}$, is then shifted by a frequency increment, $\sum_{k=2}^{n}\alpha_{k-1}t_0^{(k-1)}$, and, finally, is subject to the STFT with window $w_{(\sigma)}$. Obviously, the frequency resolution of the PCT at the specific moment t_0 is determined by both the value range of $IF_s(t) - \sum_{k=2}^{n+1}\alpha_{k-1}t^{(k-1)}$ at the time span $[t_0 - \sigma/2, t_0 + \sigma/2]$, denoted as $\Delta IF_s(t_0; \sigma)$, and the frequency bandwidth of the Gaussian window $1/\sigma$, i.e., the frequency resolution at t_0 is equal to $\Delta IF_s(t_0; \sigma) + 1/\sigma$. Ideally, if the IF trajectory of the nonlinear chirp kernel exactly matches the curve of the signal, then $IF_s(t) - \sum_{k=2}^{n+1}\alpha_{k-1}t^{(k-1)}$ will be a constant ω_0, so the value range $\Delta IF_s(t_0; \sigma)$ is zero over the whole time span, and therefore, the frequency resolutions of the PCT at all specific moments are equal to $1/\sigma$.

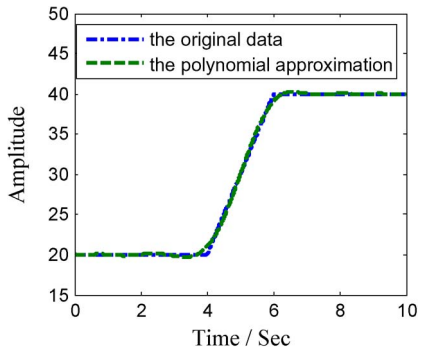

Fig. 4. Polynomial approximation of a steplike function.

Because the Weierstrass approximation theorem [25] guarantees that any continuous function on a closed and bounded interval can be uniformly approximated on that interval by a polynomial to any degree of accuracy, for example, by using the least square method, the steplike function shown in Fig. 4 can be well approximated by a polynomial function of order 15 such that

$$f(t) \approx \alpha_0 + \sum_{k=1}^{15} \alpha_k t^k \tag{11}$$

with

$$\begin{aligned}(\alpha_0, \alpha_1, \ldots, \alpha_{15}) &= (20.587702713821269, -9.051647867114209, \\ &\quad 33.245679054901196, -50.867553236045595, \\ &\quad 39.838257945911643, -17.459085588666149, \\ &\quad 4.374780231656408, -0.593065684358347, \\ &\quad 0.033494986306404, 0.000038685263729, \\ &\quad 0.000195319871483, -0.000054193791259, \\ &\quad 0.000002817176603, 0.000000194295633, \\ &\quad -0.000000023866664, 0.000000000655585).\end{aligned}$$

Therefore, given a properly selected set of parameters $(\alpha_1, \ldots, \alpha_n)$, the PCT is capable of producing a highly accurate analysis for a wide range of signals whose IF trajectories can be any continuous function of time.

C. Numerical Experiment Tests

The performance of the proposed PCT is assessed by tests on two numerically generated signals. The first signal is given as

$$s(t) = \sin\left(2\pi\left(10t + \frac{5}{4}t^2 + \frac{1}{9}t^3 - \frac{1}{160}t^4\right)\right) \quad (0 \le t \le 15). \tag{12}$$

The signal is sampled at a sampling frequency of 200 Hz. The IF trajectory of this signal is a nonlinear function of time, i.e., $f(t) = 10 + 2.5t + t^2/3 - t^3/40$ (Hz). The TFDs of the signal shown in Figs. 5(a)–(c) and 6 are generated by the conventional STFT, the CT, and the proposed PCT, respectively. In the CT, the chirp rate is taken as 6π, and in the PCT, the polynomial kernel characteristic parameters are taken as $(\alpha_1, \ldots, \alpha_3) = (5\pi, 2\pi/3, -\pi/20)$; hereby, the polynomial kernel can exactly track the curve of the IF trajectory of the signal. Basically, all the three TFDs could render the inherent time–frequency pattern of the signal. However, it is obvious that the TFD generated by the PCT has the best concentration while the TFD by the STFT has the worst concentration. In addition, it can be seen that, for the CT, the TFD's concentration at 0–10 s is better than that at 10–15 s; this is mainly due to that the IF trajectory of the signal over the time span of [0, 10] s can be well approximated by a linear chirp signal whose frequency increases with time at a speed of 3 Hz/s.

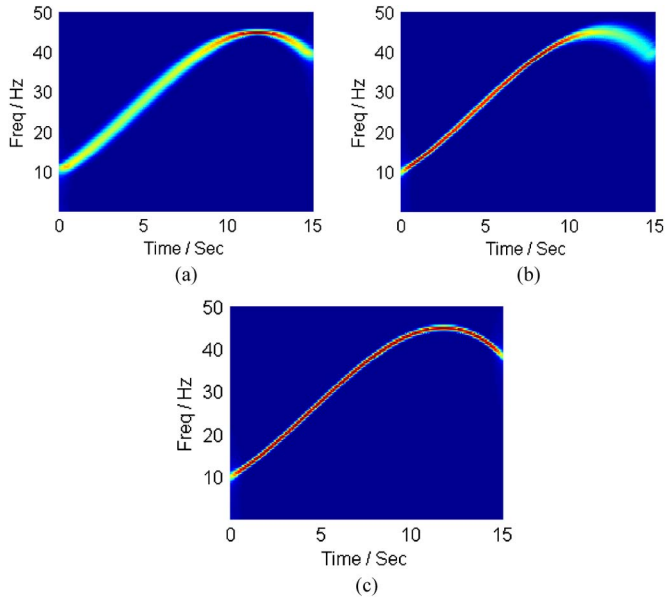

Fig. 5. TFDs of the signal given by (12) (window size $= 512$). (a) By STFT. (b) By CT. (c) By PCT.

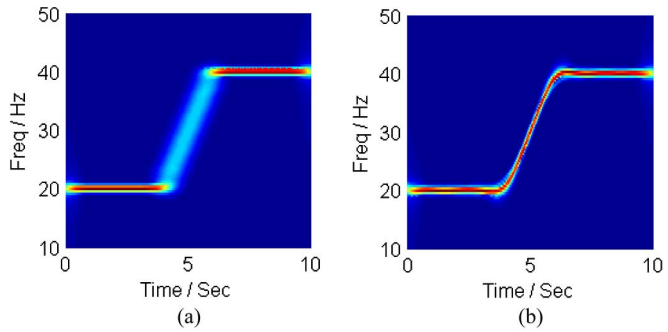

Fig. 6. TFDs of the signal with steplike IF trajectory (window size $= 512$). (a) By STFT. (b) By PCT.

The second signal considered here has an IF trajectory described by the steplike function shown in Fig. 4. Both the STFT and the PCT are used to calculate the TFD of this signal. When the PCT is used, the polynomial kernel characteristic parameters are as given in (11). It is not a surprise to see that, in this case, the PCT with a set of proper parameters produces a TFD for the signal of a much better quality in terms of concentration than the TFD analysis result by the STFT.

III. PCT-Based IF Estimation Method

As indicated by the two numerical tests in the previous section, given a set of properly determined polynomial kernel characteristic parameters, the PCT could produce a high-quality TFD for a considered signal. The result can have an excellent concentration, and the IF trajectory can be easily identified from the analysis. Therefore, the determination of proper parameters is critical for the application of the PCT method. In this section, an IF estimation method is developed by using the PCT.

Briefly speaking, the basic idea of the PCT-based IF estimation method is to use the PCT with all polynomial kernel characteristic parameters $(\alpha_1, \ldots, \alpha_n) = 0$ to roughly estimate an IF, then to approximate the roughly estimated IF using a polynomial function by the least square method, and then to conduct the PCT using the polynomial kernel characteristic parameters for the analyzed signal. Finally, the IF of the signal can be extracted from the TFD produced by the PCT. As indicated in the previous section, the more the polynomial kernels used in the PCT match the IF trajectory of the signal under consideration, the better the concentration of the TFD would be. Therefore, it is likely that the polynomial kernel estimated from the roughly estimated IF does not match the IF very well, but surely, the IF extracted from the PCT would match the true IF better than the roughly estimated IF. Therefore, we can refine the IF estimation by adjusting the polynomial kernel using the IF obtained by the PCT and conducting the PCT again using the new polynomial kernel. The procedure can be repeated until no evident modification is observed in the concentration of the TFD by the PCT or in the estimated IF.

When the concentration of the TFD is used as the criterion, the Renyi entropy can be used to measure the concentration, which is defined as

$$REN(s) = -\iint \log |PCT_s(t,\omega)|^3 \, dt \, d\omega \tag{13}$$

and the termination condition can be set as

$$\xi_{(s)} = \left| REN_{(i+1)}(s) - REN_{(i)}(s) \right| < \delta \tag{14}$$

or

$$\xi_{(s)} = \frac{\left| REN_{(i+1)}(s) - REN_{(i)}(s) \right|}{\left| REN_{(i+1)}(s) \right|} < \delta \tag{15}$$

where δ is a predetermined threshold.

When the estimated IF is used as the criterion, the termination condition is suggested as

$$\xi_{(s)} = mean\left(\int \frac{\left| IF_{(i+1)}(t) - IF_{(i)}(t) \right|}{\left| IF_{(i)}(t) \right|} dt \right) < \delta. \tag{16}$$

A. If Estimation Algorithm

The algorithm for the IF estimation can be summarized as follows.

Initial Step:

Set δ as a specific value; Set the polynomial order n; Set $(\alpha_1, \ldots, \alpha_n) = 0$; Set the window size;

The *k*th Step:

1) Calculate the PCT with $(\alpha_1, \ldots, \alpha_n)$, and denote the result as $TFD_{(k)}$;
2) Locate the peak in the $TFD_{(k)}$;
3) Approximate the TFD peak data with a polynomial function of order n using the least square method, and denote the coefficients as $(\bar{\alpha}_0, \bar{\alpha}_1, \ldots, \bar{\alpha}_n)$;
4) Calculate the termination criterion $\xi_{(s)}$;
5) If $\xi_{(s)} > \delta$, then $k = k + 1$; $(\alpha_1, \ldots, \alpha_n) = (\bar{\alpha}_1, \ldots, \bar{\alpha}_n)$ and go to 1), else go to 6);
6) Take the IF trajectory as the obtained n-order polynomial function of time;
7) Quit

As stated in the summarization, the polynomial function order needs to be predetermined at the initial step. However, it is clear that there is no information about the IF available for the signal until the first PCT is carried out. Therefore, the polynomial function order can only be initialized by trial. Usually, a relatively large order can be adopted for the polynomial function at the beginning; if the extracted TFD peak data can be well approximated with a polynomial function of relatively low order, then the estimated high-order polynomial coefficients would be close to zero.

IV. Validations

To demonstrate the effectiveness of the algorithm developed in the preceding section, the algorithm is applied to estimate the IF of the signal described by (12) and the instantaneous rotating speed of a rotor test rig from its vibration signal.

A. Numerical Signal Described by (12)

In this case, this signal is seriously contaminated by a white noise whose mean value and standard deviation are 0 and $\sqrt{3}$, respectively. When applying the PCT-based algorithm, the size of the Gaussian window is predetermined as 512, the order of the polynomial function to approximate the IF is set as four, the termination condition expressed by (16) is used, and the threshold δ is set as 0.1%.

Before the criterion has reached the threshold, four iterations of PCT have been conducted; the generated TFDs and the extracted TFD peak curves, as well as the IF estimated from the TFD peak data and the true IF, are all presented here and shown in Figs. 7–10. In Fig. 7, the PCT with $(\alpha_1, \ldots, \alpha_n) = 0$ is actually the same as the conventional STFT, and the energy of the nonlinear chirp component would be scattered over a relatively wide frequency band; thus, this component cannot show itself off very clearly in the TFD, and therefore, the extracted peaks do not match the true IF trajectory very well. Consequently, the estimated IF approximation deviates from the true IF significantly. When the polynomial coefficients of the approximation are used as the polynomial kernel characteristic parameters, the TFD concentration of the PCT is improved, as shown in Fig. 8.

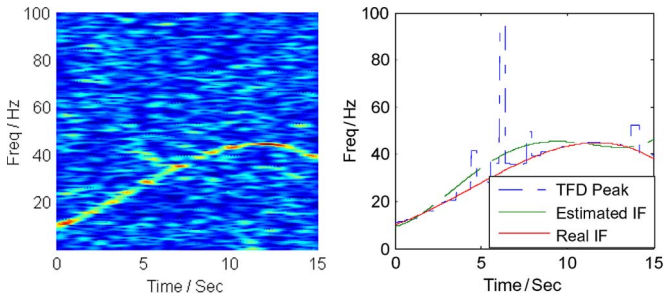

Fig. 7. TFD and the TFD peak data after the first time PCT (STFT).

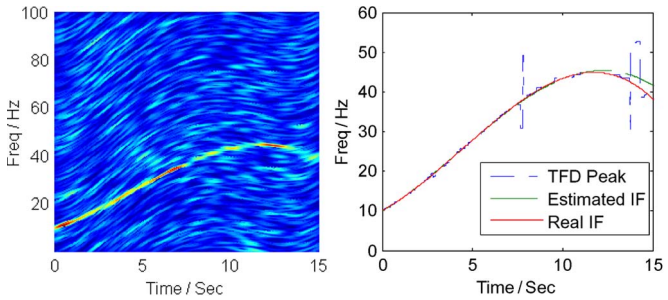

Fig. 8. TFD and the TFD peak data after the second time PCT.

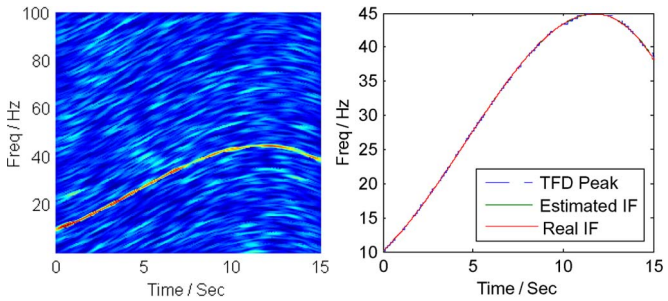

Fig. 9. TFD and the TFD peak data after the third time PCT.

Using the peak extracted from the improved TFD, the estimated IF can basically track the true IF trajectory well, except over the time span from 10 to 15 s. Again, by adopting the coefficients of the improved IF polynomial approximation, as indicated by Fig. 9, the TFD concentration for the nonlinear chirp component is significantly improved, and this component shows itself off clearly and so can be easily identified. Not surprisingly, the estimated IF could be much closer to the true IF of the nonlinear chirp signal. Now, when the polynomial chirp kernel with an IF curve that is almost the same as the IF trajectory of the signal under consideration is used in the PCT, it can be expected that the concentration of the TFD would be considerably improved for the nonlinear chirp component as the frequency bandwidth will be nearly equal to $1/\sigma$, the bandwidth of the Gaussian window. The related results are shown in Fig. 10.

The values of the calculated criterion for the termination condition are given in Table I. The results show that the criterion converges very fast. The coefficients of the polynomial function approximation are given in Table II. It can be seen that, at $k = 1$ (for the STFT), there are evident deviations between the estimated coefficients and the true values, but the deviation reduces with the increase of k, and at $k = 4$, the estimated coefficients are much closer to the true values. The relative estimating errors

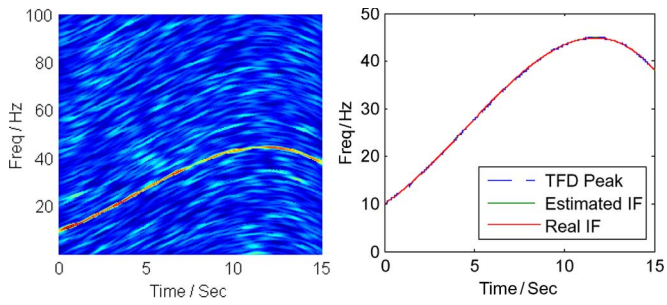

Fig. 10. TFD and the TFD peak data after the fourth time PCT.

TABLE I
VALUES OF CRITERION

$(k, k+1)$	(1, 2)	(2,3)	(3,4)
$\xi_{(s)}(\%)$	9.1345	1.0578	0.0632
Threshold δ	0.1 %		

TABLE II
ESTIMATED COEFFICIENTS OF THE POLYNOMIAL APPROXIMATION

k	1	2	3	4	True value
α_0	9.2003	9.8622	10.0148	9.9968	10.0000
α_1	1.6899	2.6237	2.4740	2.5126	2.5000
α_2	1.4300	0.3200	0.3442	0.3286	0.3333
α_3	-0.1877	-0.0274	-0.0264	-0.0244	-0.0250
α_4	0.0064	0.0003	0.0001	0.0000	0.0000

TABLE III
ESTIMATION ERROR OF THE IF

k	1	2	3	4
Error (%)	10.5568	1.1091	0.0483	0.0206

of the IF are presented in Table III. The error of 0.0206% between the final estimated IF and the true IF validates that the proposed PCT-based algorithm is able to exactly construct the IF for the signals under consideration, even under a strong noise environment. The relative error is defined as follows:

$$Error = mean\left(\int \left|\frac{IF_{(i)}(t) - IF(t)}{IF(t)}\right| dt\right). \qquad (17)$$

B. Vibration Signal Collected From a Test Rig

The analysis of the vibration signals collected during the speedup process or during the speed-down process has played an important role in the condition monitoring for rotary machines as those signals usually contain rich information about the machines' health condition. Here, the proposed PCT method is applied to estimate the instantaneous rotating speed

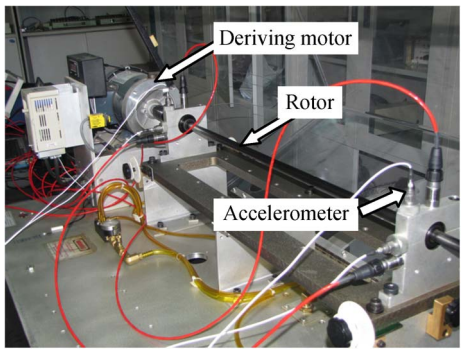

Fig. 11. Rotor test rig.

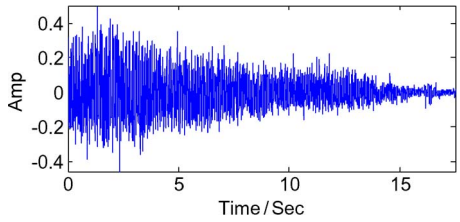

Fig. 12. Set of vibration signals.

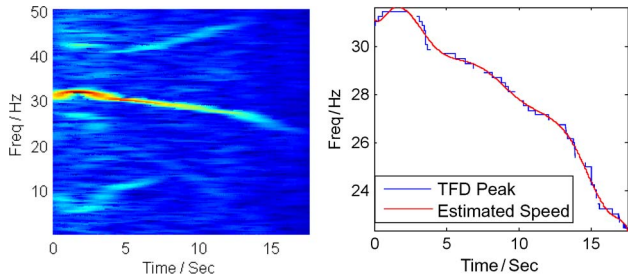

Fig. 13. TFD and the TFD peak data by the first time PCT (STFT).

of a test rig undergoing a speed-down process through the vibration signal collected with accelerometers. The test rig is shown in Fig. 11.

Fig. 12 gives a set of vibration signals to be analyzed, which was collected with the sampling frequency of 100 Hz. When applying the PCT-based algorithm, the size of the Gaussian window is predetermined as 512, the order of the polynomial kernel is set as nine, the termination condition (16) is used, and the threshold δ is set as 0.1%. Before the criterion has reached the predetermined threshold, three iterations of PCT have been implemented. Figs. 13 and 14 show the generated TFDs and the extracted TFD peak curves, as well as the estimated speed from the TFD peak data, for the first and third iterations, respectively. Obviously, the concentration of the time–frequency representation for the fundamental component in Fig. 14 is much better than that in Fig. 13 which is essentially produced by the STFT. With the estimated coefficients of the polynomial function, the instantaneous speed of the rotor undergoing a speed-down process is approximated as

$$IS(t) \approx 30.6692 - 0.1367t + 2.0530t^2 - 1.6297t^3 + 0.5266t^4 - 0.0905t^5 + 0.0090t^6 - 0.0005t^7 \text{ (Hz)}.$$

It is worth noting here that the proposed PCT would be less capable in analyzing the multicomponent signals that

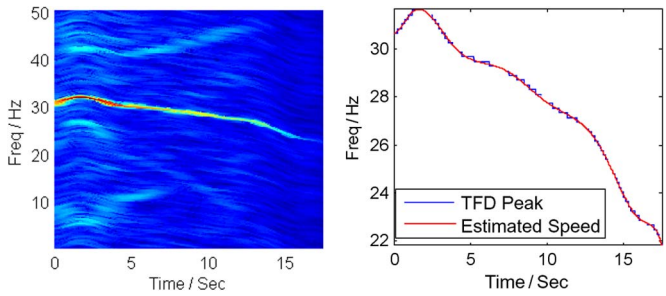

Fig. 14. TFD and the TFD peak data by the third time PCT.

contain more than one frequency components, trajectories of which have to be approximated as different polynomial functions, or at best, the PCT can track only one trajectory of the components. For example, in the analysis of the aforementioned vibration signal, except the fundamental component, the energy concentrations of the other components in the time frequency representation (TFR) generated by the PCT are even worse than that in the TFR generated by the STFT. This is a common problem for parameterized time–frequency analysis methods, including the conventional CT. Extending the PCT from the monocomponent signal to the multicomponent signal case so as to allow the PCT to be applied to a wide class of signals is the author's current research objective.

V. Conclusion

By extending the conventional CT, a new time–frequency analysis method, known as the PCT, is developed in this paper. The PCT can produce a TFD with an excellent concentration not only for the linear chirp signals, the IF of which is a linear function of time, but also for the nonlinear chirp signals, whose IF is a nonlinear function of time. In addition, based on the new developed PCT, an effective algorithm is proposed to estimate the IFs of signals, and the effectiveness of this algorithm is validated by applying this algorithm to estimate the IF of a signal with a nonlinear chirp component and seriously contaminated by a Gaussian noise and a vibration signal collected from a rotor test rig.

References

[1] J. Carson and T. Fry, "Variable frequency electric circuit theory with application to the theory of frequency modulation," *Bell Syst. Tech. J.*, vol. 16, no. 4, pp. 513–540, Oct. 1937.
[2] B. Van der Pol, "The fundamental principles of frequency modulation," *J. Inst. Elect. Eng. (London)*, vol. 93, pt. 3, no. 23, pp. 153–158, May 1946.
[3] D. Gabor, "Theory of communication," *J. Inst. Elect. Eng. (London)*, vol. 93, pt. 3, pp. 429–457, 1946.
[4] J. Ville, "Theory and applications of the notion of complex signal," RAND Corp., Santa Monica, CA, Tech. Rep. T-92, 1958.
[5] V. C. Chen and H. Ling, *Time–Frequency Transforms for Radar Imaging and Signal Analysis*. Norwood, MA: Artech House, 2002.
[6] L. R. LeBlanc, S. Panda, and S. G. Schock, "Sonar attenuation modeling for classification of marine sediments," *J. Acoust. Soc. Amer.*, vol. 91, no. 1, pp. 116–126, Jan. 1992.
[7] A. Georgakis, L. K. Stergioulas, and G. Giakas, "Fatigue analysis of the surface EMG signal in isometric constant force contractions using the averaged instantaneous frequency," *IEEE Trans. Biomed. Eng.*, vol. 50, no. 2, pp. 262–265, Feb. 2003.
[8] Y. H. Wang, "Seismic time–frequency spectral decomposition by matching pursuit," *Geophysics*, vol. 72, no. 1, pp. V13–V20, 2007.

[9] A. de Cheveigné and H. Kawahara, "YIN, a fundamental frequency estimator for speech and music," *J. Acoust. Soc. Amer.*, vol. 111, no. 4, pp. 1917–1930, Apr. 2002.
[10] L. J. Stankovic and J. Böhme, "Time–frequency analysis of multiple resonances in combustion engine signals," *Signal Process.*, vol. 79, no. 1, pp. 15–28, Nov. 1999.
[11] B. Boashash, "Estimating and interpreting the instantaneous frequency of a signal—Part I: Fundamentals," *Proc. IEEE*, vol. 80, no. 4, pp. 520–538, Apr. 1992.
[12] B. Boashash, "Estimating and interpreting the instantaneous frequency of a signal—Part II: Algorithms and applications," *Proc. IEEE*, vol. 80, no. 4, pp. 540–568, Apr. 1992.
[13] B. Boashash, P. O'Shea, and M. Arnold, "Algorithms for instantaneous frequency estimation: A comparative study," in *Proc. SPIE Conf. Adv. Algorithms Architectures Signal Process. V*, San Diego, CA, Jul. 1990, vol. 1348, pp. 126–148.
[14] R. A. Scheper and A. Teolis, "Cramer–Rao bounds for wavelet transform-based instantaneous frequency estimates," *IEEE Trans. Signal Process.*, vol. 51, no. 6, pp. 1593–1603, Jun. 2003.
[15] J. D. Harrop, S. N. Taraskin, and S. R. Elliott, "Instantaneous frequency and amplitude identification using wavelets: Application to glass structure," *Phys. Rev. E*, vol. 66, no. 2, p. 026703, Aug. 2002.
[16] L. J. Stankovi, I. Djurovi, and R. M. Lakovi, "Instantaneous frequency estimation by using the Wigner distribution and linear interpolation," *Signal Process.*, vol. 83, no. 3, pp. 483–491, Mar. 2003.
[17] E. Odegard, R. G. Baraniuk, and K. L. Oehler, "Instantaneous frequency estimation using the reassignment method," in *Proc. 68th SEG Meeting*, New Orleans, LA, 1998.
[18] L. Stankovic and V. Katkovnik, "The Wigner distribution of noisy signals with adaptive time–frequency varying window," *IEEE Trans. Signal Process.*, vol. 47, no. 4, pp. 1099–1108, Apr. 1999.
[19] V. Katkovnik and L. Stankovic, "Instantaneous frequency estimation using the Wigner distribution with varying and data-driven window length," *IEEE Trans. Signal Process.*, vol. 46, no. 9, pp. 2315–2325, Sep. 1998.
[20] B. Barkat and B. Boashash, "Instantaneous frequency estimation of polynomial FM signals using the peak of the PWVD: Statistical performance in the presence of additive Gaussian noise," *IEEE Trans. Signal Process.*, vol. 47, no. 9, pp. 2480–2490, Sep. 1999.
[21] S. C. Sekhar and T. V. Sreenivas, "Effect of interpolation on PWVD computation and instantaneous frequency estimation," *Signal Process.*, vol. 84, no. 1, pp. 107–116, Jan. 2004.
[22] P. Shui, Z. Bao, and H. Su, "Nonparametric detection of FM signals using time–frequency ridge energy," *IEEE Trans. Signal Process.*, vol. 56, no. 5, pp. 1749–1760, May 2008.
[23] S. Mann and S. Haykin, "The chirplet transform: Physical considerations," *IEEE Trans. Signal Process.*, vol. 43, no. 1, pp. 2745–2761, Nov. 1995.
[24] E. Chassande-Mottin and A. Pai, "Best chirplet chain: Near-optimal detection of gravitational wave chirps," *Phys. Rev. D*, vol. 73, no. 4, pp. 042003-1–042003-23, Feb. 2006.
[25] L. Angrisani and M. D'Arco, "A measurement method based on a modified version of the chirplet transform for instantaneous frequency estimation," *IEEE Trans. Instrumen. Meas.*, vol. 51, no. 4, pp. 704–711, Aug. 2002.
[26] [Online]. Available: http://mathworld.wolfram.com/WeierstrassApproximationTheorem.html
[27] B. Dugnol, C. Fernandez, G. Galiano, and J. Velasco, "On a chirplet transform-based method applied to separating and counting wolf howls," *Signal Process.*, vol. 88, no. 7, pp. 1817–1826, Jul. 2008.

Z. K. Peng received the B.Sc. and Ph.D. degrees from Tsinghua University, Beijing, China, in 1998 and 2002, respectively.

From 2003 to 2004, he was with the City University of Hong Kong, Kowloon, Hong Kong, as a Research Associate, and then, he was with Cranfield University, Cranfield, U.K., as a Research Officer. After that, he was with the University of Sheffield, Sheffield, U.K., for four years. He is currently a Research Professor with the State Key Laboratory of Mechanical System and Vibration, Shanghai Jiao Tong University, Shanghai, China. His main expertise relates to the subject areas of nonlinear vibration, signal processing and condition monitoring, and fault diagnosis for machines and structures.

G. Meng received the Ph.D. degree from Northwestern Polytechnical University, Xi'an, China, in 1988.

In 1993, He was a Professor and the Director of Vibration Engineering Institute with Northwestern Polytechnical University. From 1989 to 1993, he was also a Research Assistant with Texas A&M University, College Station, an Alexander von Humboldt Fellow with Technical University Berlin, Berlin, Germany, and a Research Fellow with New South Wales University, Sydney, Australia. From 2000 to 2008, he was with Shanghai Jiao Tong University, Shanghai, China, as the Cheung Kong Chair Professor, the Associate Dean, and the Dean of the School of Mechanical Engineering. He is currently a Professor and the Director of the State Key Laboratory of Mechanical System and Vibration, Shanghai Jiao Tong University. His research interests include dynamics and vibration control of mechanical systems, nonlinear vibration, and microelectromechanical systems.

F. L. Chu received the B.S. degree from the Jiangxi University of Science and Technology, Ganzhou, China, the M.S. degree from Tianjin University, Tianjin, China, and the Ph.D. degree from Southampton University, Southampton, U.K.

He is currently a Professor of mechanical engineering with the Department of Precision Instruments and Mechanology, Tsinghua University, Beijing, China. His research interests include rotating machinery dynamics, machine condition monitoring and fault detection, nonlinear vibration, and vibration control.

Z. Q. Lang received the B.S. and M.Sc. degrees from Northeastern University, Shenyang, China, and the Ph.D. degree from the University of Sheffield, Sheffield, U.K.

He is currently a Reader with the Department of Automatic Control and Systems Engineering, University of Sheffield. His main expertise relates to the subject areas of vibration control, modeling, identification and signal processing, nonlinear system frequency domain analysis and design, and monitoring and fault diagnosis for engineering systems and structures.

W. M. Zhang was born in May 1978. He received the B.S. degree in mechanical engineering and the M.S. degree in mechanical design and theories from Southern Yangtze University, Wuxi, China, in 2000 and 2003, respectively, and the Ph.D. degree in mechanical engineering from Shanghai Jiao Tong University, Shanghai, China, in 2006.

He is currently an Associated Professor with the State Key Laboratory of Mechanical System and Vibration, School of Mechanical Engineering, Shanghai Jiao Tong University. He has deep experiences in the dynamics and control for micro/nanoelectromechanical systems (MEMS/NEMS). His researches involve nonlinear dynamics and chaos control, nonlinear vibration and control, coupled parametrically excited microresonators, and the reliability analysis and assessment for MEMS/NEMS applications.

Y. Yang received the B.S. and M.S. degrees in mechanical engineering from Shanghai Jiao Tong University, Shanghai, China, in 2006 and 2009, respectively, where she is currently working toward the Ph.D. degree in the Mechanical Engineering Department. She studied at the Intelligent Maintenance System Center, University of Cincinnati, Cincinnati, OH, from 2007 to 2008.

She is currently with the State Key Laboratory of Mechanical System and Vibration, Shanghai Jiao Tong University. Her research interests include signal processing, machine health diagnosis, and prognostics.